The PD-L1/4-1BB Bispecific Antibody–Anticalin Fusion Protein PRS-344/S095012 Elicits Strong T-Cell Stimulation in a Tumor-Localized Manner

Janet K. Peper-Gabriel[1], Marina Pavlidou[1], Lucia Pattarini[2], Aizea Morales-Kastresana[1], Thomas J. Jaquin[1], Catherine Gallou[2], Eva-Maria Hansbauer[1], Marleen Richter[1], Helene Lelievre[3], Alix Scholer-Dahirel[3], Birgit Bossenmaier[1], Celine Sancerne[2], Matthieu Riviere[2], Maximilien Grandclaudon[2], Markus Zettl[1], Rachida S. Bel Aiba[1], Christine Rothe[1], Veronique Blanc[2], and Shane A. Olwill[1]

ABSTRACT

Purpose: While patients responding to checkpoint blockade often achieve remarkable clinical responses, there is still significant unmet need due to resistant or refractory tumors. A combination of checkpoint blockade with further T-cell stimulation mediated by 4-1BB agonism may increase response rates and durability of response. A bispecific molecule that blocks the programmed cell death 1 (PD-1)/programmed cell death 1 ligand 1 (PD-L1) axis and localizes 4-1BB costimulation to a PD-L1–positive (PD-L1$^+$) tumor microenvironment (TME) or tumor draining lymph nodes could maximize antitumor immunity and increase the therapeutic window beyond what has been reported for anti–4-1BB mAbs.

Experimental Design: We generated and characterized the PD-L1/4-1BB bispecific molecule PRS-344/S095012 for target binding and functional activity in multiple relevant *in vitro* assays. Transgenic mice expressing human 4-1BB were transplanted with human PD-L1–expressing murine MC38 cells to assess *in vivo* antitumoral activity.

Results: PRS-344/S095012 bound to its targets with high affinity and efficiently blocked the PD-1/PD-L1 pathway, and PRS-344/S095012-mediated 4-1BB costimulation was strictly PD-L1 dependent. We demonstrated a synergistic effect of both pathways on T-cell stimulation with the bispecific PRS-344/S095012 being more potent than the combination of mAbs. PRS-344/S095012 augmented CD4-positive (CD4$^+$) and CD8-positive (CD8$^+$) T-cell effector functions and enhanced antigen-specific T-cell stimulation. Finally, PRS-344/S095012 demonstrated strong antitumoral efficacy in an anti–PD-L1–resistant mouse model in which soluble 4-1BB was detected as an early marker for 4-1BB agonist activity.

Conclusions: The PD-L1/4-1BB bispecific PRS-344/S095012 efficiently combines checkpoint blockade with a tumor-localized 4-1BB–mediated stimulation burst to antigen-specific T cells, more potent than the combination of mAbs, supporting the advancement of PRS-344/S095012 toward clinical development.

See related commentary by Shu et al., p. 3182

Introduction

The clinical success of immune checkpoint inhibitors, particularly antibodies blocking the programmed cell death 1 (PD-1)/programmed cell death 1 ligand 1 (PD-L1) pathway, has fundamentally changed the treatment of various advanced solid cancers, such as melanoma, bladder, and non–small cell lung carcinoma (1–3). While patients who respond to anti–PD-1/PD-L1 mAb monotherapy can achieve durable clinical responses, there is still significant unmet need due to e.g., checkpoint refractory or resistant patients. Substantial efforts are being made to identify novel biologic agents and patient stratification methods that increase the fraction of patients responding to immunotherapy. While it is hypothesized that blocking the PD-1/PD-L1 pathway is "releasing the brakes" of T cells, we believe that the antitumor response could be further augmented by enhancing T-cell activation through 4-1BB–mediated costimulation.

4-1BB (CD137) is a costimulatory immune receptor belonging to the tumor necrosis factor receptor (TNFR) superfamily and is expressed on activated immune cells, including T cells (4). On T cells, 4-1BB is transiently expressed after T-cell receptor (TCR) engagement. Binding of 4-1BBL or agonistic anti–4-1BB antibodies increases T-cell effector functions, including cytokine release and cytotoxicity, as well as proliferation, survival, and memory formation (5, 6). It has been further described to modulate the metabolic reprograming of T cells (7, 8) and to mediate reinvigoration of exhausted CD8-positive (CD8$^+$) tumor-infiltrating lymphocytes (TIL; ref. 9).

The potential of 4-1BB costimulation as effective cancer immunotherapy has been extensively demonstrated in multiple preclinical studies (10–14) and is further supported by clinical data from adoptive chimeric antigen receptor (CAR) T-cell therapy validating that 4-1BB signaling elements in the cytoplasmic domain of CAR molecules are a prerequisite for durable and effective clinical responses (15, 16). Agonistic anti–4-1BB mAbs, such as urelumab (17) and utomilumab (18, 19) were clinically tested, yet did not advance to later stage clinical trials. While severe liver toxicity was reported for

[1]Pieris Pharmaceuticals GmbH, Hallbergmoos, Germany. [2]Institut de Recherches Servier, Center for Therapeutic Innovation Oncology, Croissy-sur-Seine, France. [3]Institut de Recherches Internationales Servier Oncology R&D Unit, Suresnes, France.

Current address for M. Grandclaudon: Department of Medical Oncology, Dana-Farber Cancer Institute, Boston, Massachusetts.

Corresponding Author: Janet K. Peper-Gabriel, Pieris Pharmaceuticals GmbH, Zeppelinstrasse 3, Hallbergmoos 85399, Germany. Phone: 0049-811-124470; E-mail: peper@pieris.com

Clin Cancer Res 2022;28:3387–99

doi: 10.1158/1078-0432.CCR-21-2762

Translational Relevance

Resistance to immunotherapy is common in patients with cancer. To develop a more potent immune modulator, we combined 4-1BB activation and programmed cell death 1 ligand 1 (PD-L1) checkpoint inhibition in a novel bispecific format. The PD-L1/4-1BB bispecific PRS-344/S095012 was generated by fusing a 4-1BB–targeting Anticalin protein to a PD-L1–specific antibody to promote PD-L1–dependent 4-1BB activation. This offers the clinical advantage of localizing 4-1BB engagement to PD-L1–positive tissues like the tumor microenvironment, promoting antitumoral immune responses while reducing the risk of peripheral 4-1BB stimulation. The *in vitro* and *in vivo* characterization we show here highlights the potential of PRS-344/S095012 to provide a novel treatment option for patients who do not benefit from current immunotherapies. Furthermore, we show that soluble 4-1BB is a specific marker of 4-1BB pathway activation by PRS-344/S095012 in *in vitro* and *in vivo* models, highlighting its potential as an exploratory biomarker in patients.

urelumab (20), utomilumab monotherapy showed only limited preliminary antitumor activity (21), which is concordant with preclinical observations indicating a potential lower stimulatory capacity compared with urelumab (22). These clinical observations suggest that efficacy of systemic 4-1BB stimulation is limited by its potential to induce severe liver toxicity.

To gain tumor specificity and reduce peripheral toxicity, we generated 4-1BB–targeting bispecific molecules designed to mediate hyperclustering of 4-1BB by binding to a tumor-localized target, thereby bridging 4-1BB–positive (4-1BB$^+$) T cells with tumor cells and inducing a potent 4-1BB signaling in the tumor microenvironment (TME). We previously described cinrebafusp alfa (PRS-343), a HER2/4-1BB bispecific molecule generated by recombinant fusion of a 4-1BB–specific Anticalin protein to an Fcγ receptor (FcγR)-silenced IgG4 variant of trastuzumab (23). Anticalin proteins are 18 or 21 kDa protein therapeutics engineered from human lipocalins, a family of natural extracellular binding proteins that provide several benefits, such as a compact target engagement interface, which can be engineered to bind specifically to a wide range of relevant targets, and a straightforward recombinant engineering profile. Despite low amino acid identity, lipocalins are characterized by a highly conserved, robust tertiary structure that enables the generation of multispecific molecules with high formatting flexibility (24). In a clinical phase I dose escalation study, single-agent cinrebafusp alfa demonstrated antitumor activity, including stable disease, partial and complete responses, in heavily pretreated patients across multiple HER2$^+$ tumors. Beyond demonstrating clinical benefit, cinrebafusp alfa showed strong increases in CD8$^+$ T-cell numbers and proliferative index in the TME of responders, indicative of 4-1BB agonism on T cells (25). In addition, cinrebafusp alfa was deemed safe and well tolerated as a single agent or in combination with atezolizumab, highlighting the advantage of tumor-localized 4-1BB stimulation and supporting the further development of cinrebafusp alfa for treatment of HER2$^+$ malignancies.

To expand 4-1BB agonistic opportunities beyond HER2$^+$ carcinomas, we generated PRS-344/S095012, a PD-L1/4-1BB bispecific molecule, by fusing 4-1BB–specific Anticalin proteins to a PD-L1–specific antibody, and its preclinical characterization is described in this study.

Materials and Methods

Generation of the antibody–Anticalin fusion PRS-344/S095012

The Anticalin protein J10 specifically targeting human 4-1BB with high affinity was obtained utilizing phage display selection and protein engineering as previously described (23). A humanized PD-L1 targeting mAb obtained from immunization of BALB/C mice and standard hybridoma generation was reformatted to an IgG4 backbone containing F234A, L235A, and S228P mutations. To generate PRS-344/S095012, J10 was recombinantly fused to the C-terminal heavy chain of the anti–PD-L1 mAb building block using a flexible glycine-serine linker $(G4S)_3$. PRS-344/S095012, Fc-J10 (J10 fused to an IgG4 isotype with F234A, L235A, S228P), huPD-L1-huFc-Bio, and the anti–PD-L1 mAb building block were produced from mammalian expression in CHO cells using standard techniques.

Reagents and cells

Recombinant human 4-1BB, PD-L1, huPD-1-huFc, CD80-Fc, FcγRI, FcγRIIa, and FcγRIIIa protein were obtained from R&D Systems (9220–4B; 9049-B7; 1086-PD-01M; 140-B1; 1257-FC; 1330-CD; 4325-CD), IgG4 isotype control from Sigma Aldrich (14639) and atezolizumab (Tecentriq) from Genentech, avelumab (Bavencio) from Merck, nivolumab (Opdivo) from Bristol-Myers Squibb, and trastuzumab (Herceptin) from Roche. The sequences for anti–4-1BB mAbs 20H4.9 (expected to correspond to urelumab; ref. 26), CTX-471 (27), and PF-05082566 (utomilumab; ref. 18) were extracted from patents and constructs were produced from expression in CHO cells using standard techniques.

Human colon carcinoma cell line RKO (CRL-2577; ATCC) was maintained in 90% RPMI 1640 + GlutaMAX (61870–010; Gibco), 10% FBS (F7524; Sigma-Aldrich), and 1% Pen/Strep (15140–122; Gibco). CHO cells expressing human PD-L1 or 4-1BB were established by stable transfection using the Flp-In system (Invitrogen) and cultured in Ham's F12 Nut Mix + GlutaMAX (31765–027; Gibco), 10% FBS, 1% Pen/Strep, and 500 μg/mL Hygromycin B (CP12.2; Gibco). NF-B-Luc2/4-1BB Jurkat, Jurkat_PD1_NFATLuc2, PD-L1 aAPC/CHOK1, and CHO:FcγRIIb cells (Promega) were cultured according to the manufacturer's instructions. Murine colon carcinoma MC-38 cell line was genetically engineered to knock out murine and knock in human PD-L1. MC-38-huPD-L1 (Biocytogen) were cultured in DMEM (Excell) and 10% FBS. All cells were cultured at 37°C, 5% CO_2. Authentication of human cell lines was performed by genotyping-based cell line authentification service (Eurofins). All cell lines were used within 3 months of thawing and checked for *Mycoplasma* using PCR every 3 months.

Human buffy coat samples from healthy volunteers were obtained from the Institute for Clinical Transfusion Medicine and Immunogenetics (Ulm, Germany) after obtaining written informed consent.

Peripheral blood mononuclear cells (PBMC) were isolated from buffy coats by centrifugation through a polysucrose density gradient. Cellular subsets of PBMCs were further purified by using pan–T-cell isolation kit, CD4, CD8, or CD14 MicroBeads (130–096–533, 130–096–495 and 130–050–201; Miltenyi Biotec) according to the manufacturer's instructions.

For mixed lymphocyte reaction (MLR) assays, cones remaining after platelet apheresis from healthy volunteers were obtained through the Etablissment Francais du Sang (EFS), section de Poissy-France, in line with French regulation.

Mice

Human 4-1BB knock-in mice (Hu4-1BB KI; developed and purchased from Biocytogen) are genetically engineered C57BL/6 mice in which the human 4-1BB extracellular domain is knocked in to replace the murine 4-1BB extracellular domain. Animals were housed in a temperature- and humidity- controlled specific pathogen-free (SPF) barrier at the Animal Center of Beijing Biocytogen in individual ventilated cage with 5 animals per cage. Animals were housed for at least 7 days of acclimation before the start of experiment.

ELISA

Recombinant protein of 4-1BB or PD-L1 was coated onto microtiter plates and incubated with a titration series of constructs. Binding was detected using a peroxidase-conjugated anti-human IgG Fab mAb (209–035–097; Dianova) or using an affinity purified polyclonal anti-Anticalin mAb, generated by rabbit immunization (Pieris Pharmaceuticals GmbH/Biogenes). For dual target engagement, recombinant His-tagged 4-1BB was coated onto a microtiter plate followed by the addition of test constructs. Bound molecules were detected via biotinylated PD-L1–Fc and Extravidin horseradish peroxidase (Sigma-Aldrich). For competition ELISA, His-tagged CD80-Fc was coated onto microtiter plates. Ten nanomoles per liter of huPD-L1-huFc-Bio as free tracer and a titration series of constructs was preincubated for 1 hour and then added to the CD80 coated plate. Binding was detected using a Streptavidin Sulfo-Tag (R32AD-1; MSD).

Biacore

A CM5 chip was immobilized with an anti-IgG or anti-His antibody via N-Hydroxysuccinimide and 1-Ethyl-3-(3-dimethylaminopropylcarbodiimide (EDC/NHS) chemistry using commercial capture kits (GE Lifesciences) following the distributor's instructions. Test constructs or FcγR were captured on the chip via the anti-Fc or His-tag and hu4-1BB, huPD-L1, nivolumab, trastuzumab, or PRS-344/S095012 were used as analytes. Constructs were applied in with a flow rate of 30 μL per minute. The sample contact time was 180 seconds and the dissociation time was 900 or 450 seconds. All measurements were performed at 25°C on a Biacore 8K or T200 (GE Lifesciences). The kinetics data (but not FcγR) were fitted using a 1:1 binding model using Biacore 8K evaluation software.

Flow cytometry

All steps were performed on ice or at 4°C. Cells were incubated with test constructs diluted in PBS (Gibco) + 5% FCS, followed by an incubation with anti-human IgG-Alexa488 labelled secondary antibody. Fluorescence signals were quantified using an Intellicyte iQue Screener Plus (Sartorius).

Reporter assays

For the 4-1BB/NFκB bioassay, 2.5×10^5 cells/mL of PD-L1–positive (PD-L1$^+$) target cells and 1.875×10^6 cells/mL of NFκB-Luc2/4-1BB Jurkat cells were cocultured for 4 hours in presence of test constructs. For the PD-1/NFAT bioassay, 3.2×10^5 cells/mL of PD-L1 aAPC/CHOK1 and 5×10^5 cells/mL of Jurkat_PD1_NFATLuc2 cells were cocultured for 6 hours in presence of test constructs. Bio-Glow luciferase reagent (Promega) was added and luminescence was measured as relative light units (RLU) using a luminescence plate reader (Cytation 5; Biotek). All incubation steps were performed at 37°C, 5% CO_2.

T-cell coculture assay

CHO:huPD-L1 or CHO:mock cells were treated with 10 μg/mL of mitomycin C (M4287; Sigma-Aldrich) for 30 minutes to inhibit proliferation. After washing with PBS, cells were seeded into culture plates precoated with 0.25 μg/mL anti-CD3 (OKT3; 16–0037; eBioscience). The next day, 1.25×10^6/mL T cells and test constructs were added in assay medium (RPMI 1640 + 10% FBS + 1% Pen/Strep). After 48 hours of coculture, supernatants were collected and analyzed for IL2 secretion in an electrochemiluminescence (ECL) immunoassay (Mesoscale Discovery) using an IL2 DuoSet kit (DY202; R&D Systems). All incubation steps were performed at 37°C, 5% CO_2.

Staphylococcal enterotoxin B assay

PBMCs were seeded at a cell density of 1.25×10^6 cells/mL in assay medium. PBMCs were stimulated with 0.25 ng/mL staphylococcal enterotoxin B (SEB; S4881; Sigma-Aldrich) and a titration series of constructs for 72 hours at 37°C, 5% CO_2. Supernatants were collected and analyzed for IL2 secretion as described above.

MLR assay

Freshly isolated CD14$^+$ monocytes were cultured in RPMI1640 + 10% FBS + 1% Pen/Strep + 50 ng/mL IL4 + 100 ng/mL of GM-CSF (130–093–922 and 130–093–864 both from Miltenyi Biotec) for 6 days at 2×10^6 cells/mL. At day 3, fresh medium containing cytokines were added. At day 6, monocyte-derived dendritic cells (moDC) were harvested and cultured with CD8$^+$ or CD4-positive (CD4$^+$) T cells obtained from another healthy donor in a 1:5 ratio in the presence of test constructs. All incubation steps were performed at 37°C, 5% CO_2. MLR supernatants were harvested and kept frozen at −80°C until quantification of cytokines in a luminex assay was performed. For CD4-based MLR, the HCYTOMAG-60K-04 kit (Merck) was used to quantify IL2, IFNγ, IL10, and TNFα. For CD8-based MLR, the HCD8MAG-15K-13 kit (Merck) was used to quantify IL2, IFNγ, TNFα, IL5, IL13, granzyme A, granzyme B, FasL, and perforin. Measurement was carried out using a Biorad Bioplex 200 machine and data analysis was performed with the provided software.

Antigen-specific T-cell assay

PBMCs were thawed and seeded onto six-well plates in assay medium consisting of RPMI1640 supplemented with 5% human serum (BioIVT) + 1% Pen/Strep + 25 μg/mL gentamycin (15750060; Gibco) + 50 μmol/L β-mercaptoethanol (21985023; Gibco). After overnight resting, PBMCs were seeded in assay plates and stimulated with 0.25 μg/mL of a peptide pool containing HLA-class I restricted T-cell epitopes from cytomegalovirus (CMV), Epstein–Barr virus (EBV), and influenza (CEF peptide pool; PM-CEF-E; JPT Peptide Technologies). After 48 hours, supernatants were collected and analyzed for IFNγ secretion in an ECL immunoassay using an IFNγ DuoSet kit (DY285B; R&D Systems). For antigen reexposure, PBMCs were stimulated with 1 μg/mL CEF peptide pool 1 day after thawing. IL2 (78036.3; STEMCELL technologies), 20 U/mL, was added on day 2, 5, and 7. On day 12, cells were collected and equally seeded in assay plates. 0.25 μg/mL of peptide pool and 5 nmol/L of respective constructs were added. After 48 hours, supernatants were collected and analyzed for IFNγ secretion. All incubation steps were performed at 37°C, 5% CO_2.

T-cell–mediated cytotoxicity and antibody-dependent cell-mediated cytotoxicity

RKO cells were seeded into E-Plates (5867681001; Agilent) compatible with the xCELLigence RTCA HT instrument. RKO cells were allowed to attach and proliferate for 48 hours. One day after thawing,

$CD8^+$ T cells were transferred to RKO cells in a 5:1 ratio. 0.3 μg/mL anti-CD3 antibody and 10 nmol/L of each test construct were added. For antibody-dependent cell-mediated cytotoxicity (ADCC) experiments, PBMCs were added in a 40:1 ratio without anti-CD3 antibody. Cytotoxic activity was detected as decreasing cell adhesion of RKO cells measured as unitless cell index (CI) in real-time using the RTCA HT Software V1.0.1 (ACEA Biosciences). CI values were normalized to the first measurement after adding T cells. Specific lysis was calculated using the following formula: 100 - (normalized mean CI of test molecule/normalized mean CI of isotype control) x 100. Specific killing values were exported to GraphPad Prism v8.3 and plotted over time. All incubation steps were performed at 37°C, 5% CO_2.

In vivo model

PRS-344/S095012 *in vivo* activity was evaluated in a MC38-huPD-L1 model using human 4-1BB knock-in mice (Biocytogen). Briefly, 5×10^5 MC38-huPD-L1 cells were subcutaneously injected in the right flank of hu4-1BB KI mice (males and females, aged 6–8 weeks). When tumors reached a mean value of 103 mm^3 (D0), the mice were randomized based on equivalent average tumor volume in seven groups ($n = 10$; samples sized based on pilot study data) and treatment schedule started with twice weekly intravenous injections for 3 weeks (operator blinded). Tumor growth was monitored twice weekly and tumor volume was calculated as follows: (length × $width^2$)/2. Plasma from mice was drawn in K2-EDTA tubes at indicated timepoints before drug administration. S4-1BB in plasma was detected using a custom-made assay and analyzed in the gyrolab platform. All animal studies were performed following ethical protocols reviewed and approved by the Institutional Animal Care and Use Committee (IACUC) of Biocytogen in accordance with the guidelines by the Association for Assessment and Accreditation of Laboratory Animal Care (AAALAC).

Statistical analysis

Nonlinear regression was performed using a sigmoidal 4-parameter dose-response model (GraphPad Prism v8.3). All graphs and statistical analysis were generated using GraphPad Prism v8.3 software. Values of $^* = P < 0.05$; $^{**} = P < 0.01$; $^{***} = P < 0.001$ were considered significant.

Data availability

The data generated in this study are available upon request from the corresponding author.

Results

Generation and binding characteristics of PRS-344/S095012

To combine PD-1/PD-L1 pathway blockade with PD-L1–dependent 4-1BB costimulation, the PD-L1/4-1BB bispecific molecule PRS-344/S095012 was generated by fusing the human 4-1BB targeting Anticalin protein J10 with an anti–PD-L1 antibody. We selected an IgG4 isotype with the hinge stabilizing mutation S228P (28), as well as F234A and L235A mutations to reduce binding to FcγRs and to avoid FcγR-mediated effector functions, while maintaining FcRn binding (29). J10 was fused via a glycine-serine linker to the C-terminus of the antibody heavy chain (**Fig. 1A**), resulting in a bivalent binding mode of PRS-344/S095012 towards both targets requiring further hyperclustering mediated by PD-L1 binding to induce 4-1BB activation.

PRS-344/S095012 demonstrated no significant binding to FcγRI, FcγRIIA, and FcγRIIIA in a surface plasmon resonance (SPR) assay, as expected (Supplementary Fig. S1A–S1C). In line with lack of effector function in the Fc part, PRS-344/S095012 did not show ADCC activity on PD-$L1^+$ cells (Supplementary Fig. S1D).

PRS-S344/S095012 demonstrated binding to recombinant human 4-1BB and PD-L1 (**Fig. 1B** and **C**) with EC_{50} values each in the subnanomolar range (4-1BB: 0.29 ± 0.02 nmol/L; PD-L1: 0.61 ± 0.01 nmol/L; mean ± SEM). Binding affinities were comparable with the respective building blocks and simultaneous binding to both targets was shown in dual target binding ELISA experiments (**Fig. 1D**; EC_{50}: 1.3 ± 0.06 nmol/L; mean ± SEM). SPR experiments of PRS-344/S095012 demonstrated binding to human 4-1BB and PD-L1 with a KD of 4.84 ± 0.24 nmol/L and 0.68 ± 0.14 nmol/L (mean ± SD), respectively (representative SPR sensorgrams and kinetic parameters in Supplementary Fig. S2A–S2E). Comparable with atezolizumab and recombinant PD-1, PRS-344/S095012 and the anti–PD-L1 mAb building block inhibit the interaction of CD80 with PD-L1 (Supplementary Fig. S2F). In flow cytometry experiments using transfected CHO cells, we confirmed binding to cellular expressed human 4-1BB and PD-L1 with EC_{50} values in the low nanomolar range (**Fig. 1E** and F; 4-1BB: 1.31 ± 0.18 nmol/L; PD-L1: 3.79 ± 1.27 nmol/L; mean ± SEM), while no binding to mock transfected, target negative cells was detected (**Fig. 1G**).

PRS-344/S095012–mediated T-cell activation is superior to the combination of anti–PD-L1 and anti–4-1BB mAbs

To demonstrate that PRS-344/S095012 can combine PD-L1–dependent 4-1BB costimulation with PD-1/PD-L1 checkpoint blockade, we confirmed both activities independently. First, checkpoint blockade activity was assessed by coculturing PD-L1–expressing cells with PD-1–overexpressing Jurkat cells having an NFAT luciferase reporter gene. Addition of PRS-344/S095012 to the coculture significantly enhanced NFAT signaling, which is comparable with the anti–PD-L1 mAb building block and the anti–PD-L1 mAb atezolizumab demonstrating effective blockade of the PD-1/PD-L1 pathway (**Fig. 2A**; EC_{50} and fold stimulation values in Supplementary Table S1).

The ability of PRS-344/S095012 to induce PD-L1–dependent 4-1BB stimulation was assessed using an NFκB-Luc2/4-1BB Jurkat cell reporter assay. In the presence of PD-$L1^+$ cells, PRS-344/S095012 enhanced NFκB activity in Jurkat cells, leading to a significant increase in luciferase activity (**Fig. 2B**). PRS-344/S095012 thereby demonstrated a significantly higher efficacy and potency than the anti–4-1BB agonistic antibody 20H4.9 alone or in combination with atezolizumab. In the absence of PD-$L1^+$ cells, PRS-344/S095012 did not induce NFκB signaling, while 20H4.9-mediated signaling was retained and comparable with the condition with PD-$L1^+$ cells (**Fig. 2C**; Supplementary Table S1). Furthermore, we demonstrated that FcγR-silenced PRS-344/S095012 does not induce 4-1BB signaling in the presence of FcγRIIb-positive cells, as expected (Supplementary Fig. S3). This is in contrast to 20H4.9 and other anti–4-1BB mAbs which have been reported to mediate FcγR-dependent 4-1BB activation (27). In this experiment, PD-L1–mediated 4-1BB activation also showed higher efficacy and potency than FcγRIIb-mediated clustering.

The ability to engage 4-1BB signaling in a strictly PD-L1–dependent manner was further confirmed using primary human T cells. T cells from healthy donors were stimulated with suboptimal doses of anti-CD3 antibody in the presence of human PD-L1–transfected CHO cells and IL2 secretion was analyzed to measure T-cell activation. PRS-344/S095012 increased IL2 secretion in a dose-dependent manner (**Fig. 2D**), that was significantly higher than the combination of 20H4.9 and atezolizumab. When cocultured with mock-transfected CHO cells, PRS-344/S095012 did not increase IL2 secretion, while

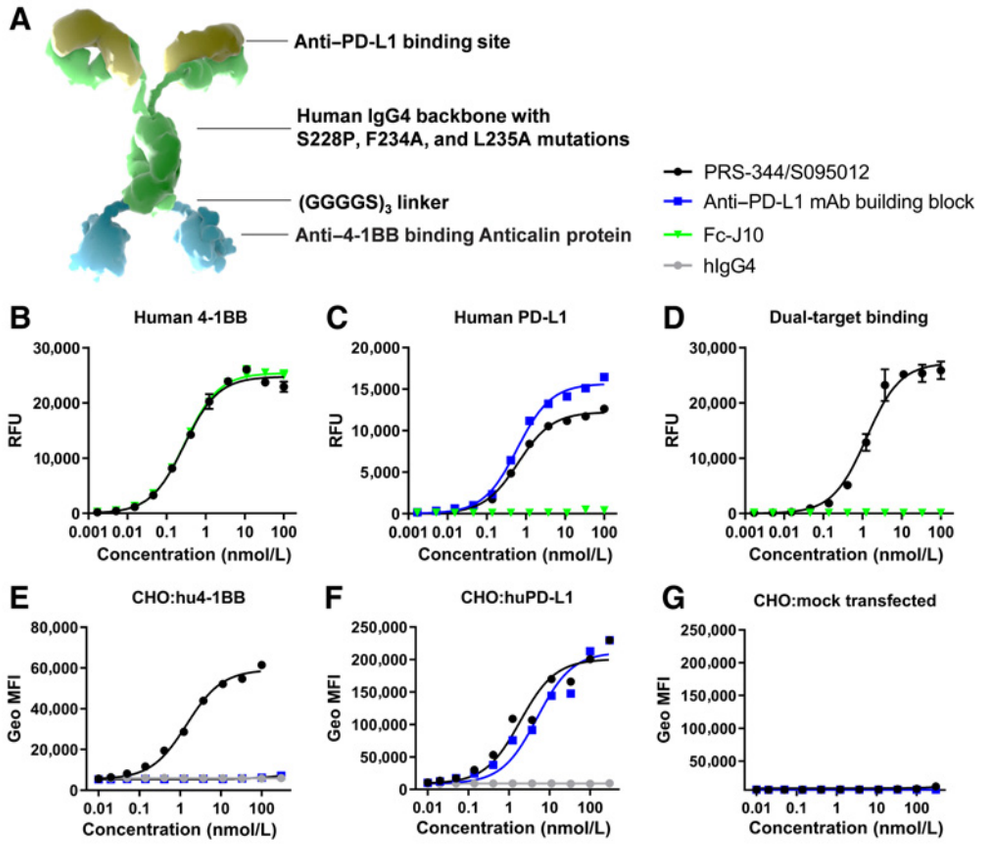

Figure 1.

Design and target engagement of PRS-344/S095012. **A,** Structure and design of PRS-344/S095012. Binding of PRS-344/S095012 to recombinant human 4-1BB (**B**) and human PD-L1 (**C**) was assessed by ELISA. **D,** Dual-target engagement was determined in dual-target binding ELISA by coating 4-1BB and detecting PD-L1 binding. Binding to cellular expressed target proteins was confirmed by FACS using CHO cells transfected with human 4-1BB (**E**), PD-L1 (**F**), or mock transfected (**G**). Data are depicted as mean ± SD. Exemplary data of three independent experiments are shown. RFU, relative fluorescence unit; MFI, mean fluorescence intensity.

activity of 20H4.9 was retained and comparable with that observed with PD-L1–expressing cells (**Fig. 2E**). Adding excess anti–PD-L1 mAb building block to the coculture with PD-L1–transfected CHO cells diminished PRS-344/S095021–mediated activation, further confirming PD-L1 dependency (Supplementary Fig. S4A). No increase in IL2 secretion was detected with any construct in the absence of anti-CD3, demonstrating that 4-1BB costimulation requires prior TCR stimulation.

Beyond PD-L1$^+$ cells, antigen-presenting cells (APC) represent a major source of PD-L1. Therefore, we assessed PRS-344/S095012 activity by stimulating healthy blood donors PBMCs with suboptimal doses of SEB to induce basal TCR stimulation. Single treatment with anti–4-1BB mAb 20H4.9 or anti–PD-L1 mAb showed only modest T-cell costimulation measured by an increase in IL2 secretion (**Fig. 3**). The combination of anti–4-1BB and anti–PD-L1 mAbs, however, significantly enhanced T-cell stimulation, demonstrating a synergistic effect of PD-L1 and 4-1BB modulation. Finally, PRS-344/S095012 resulted in superior T-cell activation compared with equimolar doses of mAb combination, indicating that the bispecific format brings a synergistic effect. Comparable results were obtained for IFNγ secretion (Supplementary Fig. S4B).

Overall, these data demonstrate that PRS-344/S095012 enhances T-cell activity only in the context of PD-L1–expressing cells, as opposed to 20H4.9, whose stimulatory properties are not restricted to the presence of PD-L1. Furthermore, stimulation via 4-1BB requires preactivated T cells, potentially focusing the activity of PRS-344/S095012 to antigen-specific T cells in the TME and avoiding toxicitis by stimulating nonactivated T cells in the periphery.

PRS-344/S095012 increases T-cell effector functions by enhancing effector molecule secretion and T-cell–mediated lysis of tumor cells

4-1BB costimulation and its synergistic effect with checkpoint blockade have been mainly described to increase CD8$^+$ T-cell effector functions. In an MLR assay of isolated CD8$^+$ T cells with allogenic moDCs, agonistic anti–4-1BB, or anti-PD-L1 mAb had only a modest impact on CD8$^+$ T-cell activation measured by the release of IFNγ, IL2, perforin, and granzyme A and B (**Fig. 4**). PRS-344/S095012 induced a T-cell response that was significantly stronger than the single treatments and superior to the combination of both mAbs. This demonstrates that PRS-344/S095012 induces a strong proinflammatory and cytotoxic CD8$^+$ T-cell phenotype and suggests that the synergistic effect of 4-1BB and PD-L1 is further enhanced by the bispecific format. Similar results were observed in MLR experiments using isolated CD4$^+$ T cells, although overall IL2 values were lower than in the CD8 MLR assay (Supplementary Fig. S5).

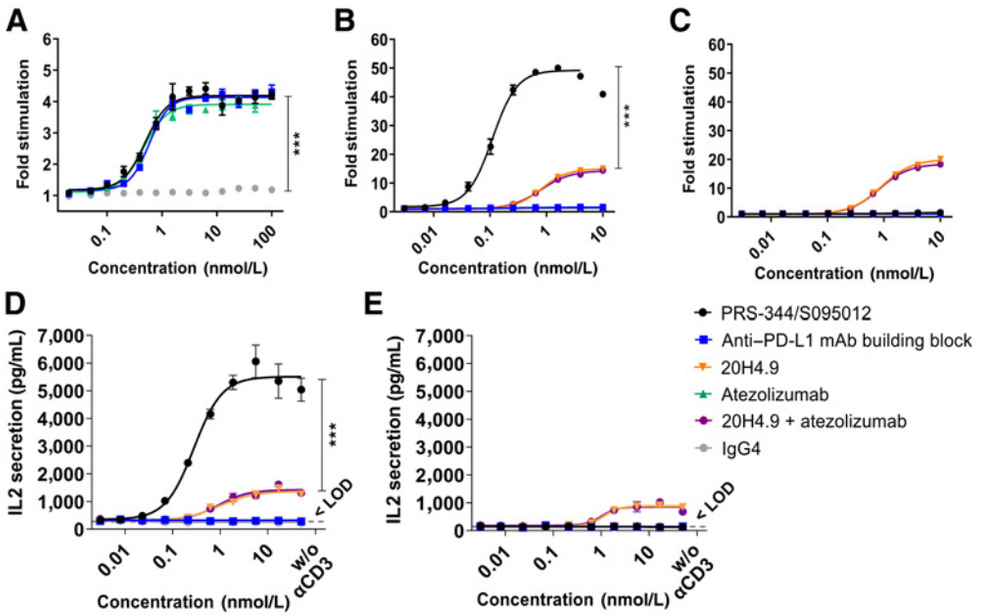

Figure 2.

PRS-344/S095012 increases T-cell stimulation by checkpoint blockade and PD-L1–dependent 4-1BB costimulation. **A,** PD-1/NFAT reporter cells were cocultured with PD-L1^{+} target cells in the presence of test constructs. 4-1BB/NF-κB reporter cells were cocultured with constructs in the presence (**B**) or absence (**C**) of PD-L1–expressing RKO cells. Luminescence activity for both reporter assays was measured in RLU and has been normalized to baseline as fold stimulation. Data are representative of three independent experiments. Primary T cells were activated with 0.25 μg/mL anti-CD3 (αCD3) and cocultured with CHO:huPD-L1 cells (**D**) or mock-transfected CHO cells (**E**). After 48 hours, IL2 secretion levels were measured. The highest concentration of each construct was additionally tested without anti-CD3 stimulation. Representative data of T cells from six different healthy blood donors are shown. <LOD, below limit of detection. Dashed lines indicate IL2 secretion in the absence of test constructs. All data are shown as mean ± SEM. Significance was calculated comparing AUC using an unpaired one-way ANOVA with Tukey multiple comparisons test.

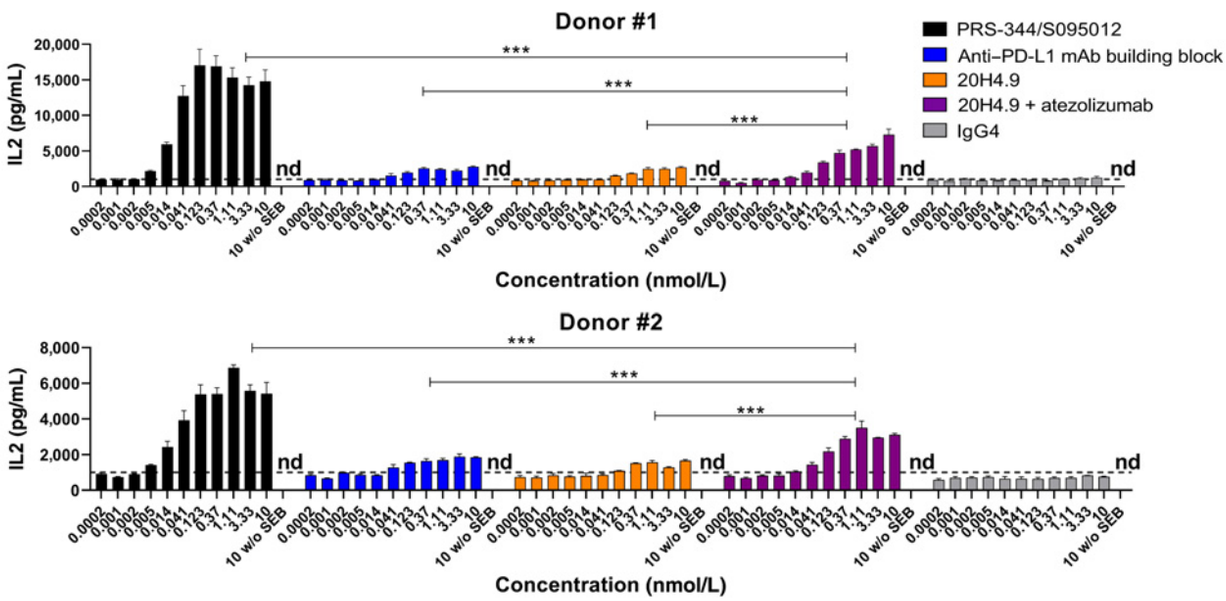

Figure 3.

PRS-344/S095012 increases T-cell activation in SEB assay. Human PBMCs were stimulated with 0.25 ng/mL SEB in the presence of indicated constructs. The highest concentration of each construct was added to unstimulated PBMC as a negative control. IL2 secretion levels were measured from the supernatant after 72 hours. Dashed lines indicate IL2 secretion of SEB-stimulated PBMCs without constructs. Data are shown as mean ± SEM. Results of two of eight tested PBMC donors are shown. nd, not detected, because values are below limit of detection. Significance was calculated comparing AUC using an unpaired one-way ANOVA with Tukey multiple comparisons test.

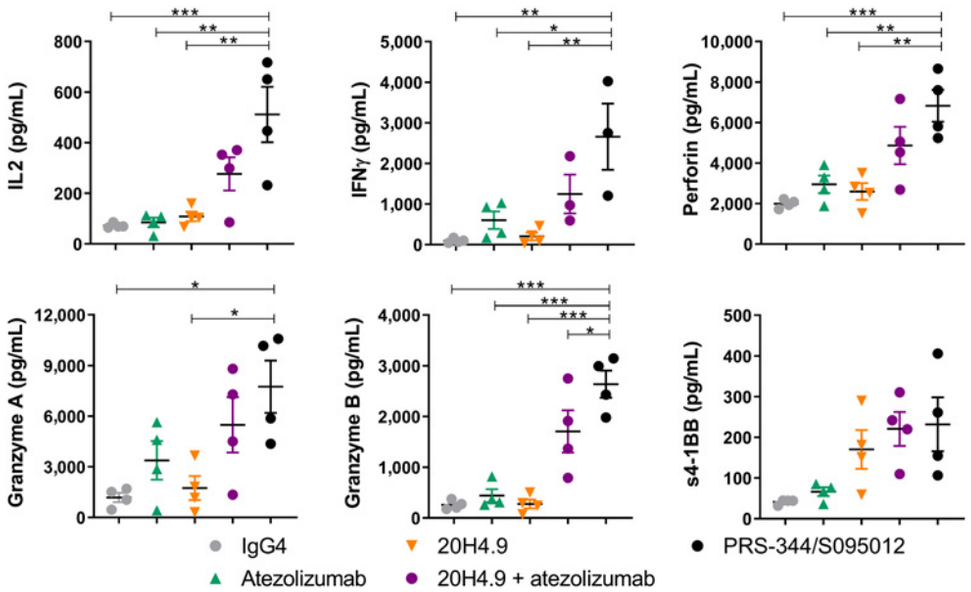

Figure 4.

PRS-344/S095012 increases CD8$^+$ T-cell effector functions in MLR experiments. CD8$^+$ T cells were cocultured with allogenic monocyte-derived dendritic cells (DC) in the presence of 1 μg/mL of indicated constructs. After 6 days, levels of effector molecules were measured using a Luminex panel. Data is shown for four individual healthy donors as mean ± SEM. Significance was calculated using an unpaired one-way ANOVA with Holm–Sidak multiple comparisons test.

In the CD8 MLR assay, we also detected the release of soluble 4-1BB (s4-1BB) after treatment with PRS-344/S095012, at levels comparable with 20H4.9 (**Figure 4**). In contrast, atezolizumab resulted in limited s4-1BB release indicating that s4-1BB allows to specifically measure the 4-1BB arm activity of PRS-344/S095012. In an independent SEB stimulation assay, PRS-344/S095012 and 20H4.9 resulted in s4-1BB increase, while binding of J10 fused to the Fc portion of an IgG4 isotype (a molecule able to bind 4-1BB but unable to induce signaling) did not lead to s4-1BB secretion (Supplementary Fig. S4C).

To further investigate the impact of PRS-344/S095012 on cytotoxic CD8$^+$ T cells, we activated primary CD8$^+$ T cells with suboptimal doses of anti-CD3 and measured the allogenic lysis of cocultured PD-L1$^+$ RKO tumor cells over time. PRS-344/S095012 further

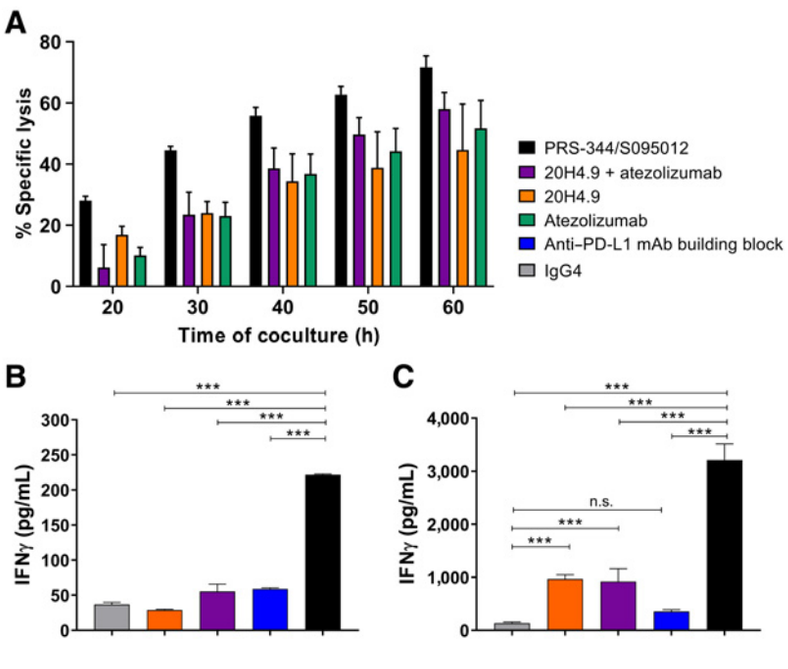

Figure 5.

PRS-344/S095012 increases T-cell–mediated lysis of PD-L1$^+$ tumor cell line and increases antigen-specific T-cell responses. **A,** RKO tumor cell line was plated to E-plates and allowed to attach. Primary human CD8$^+$ T cells were added in a 5:1 ratio and activated with 0.3 μg/mL anti-CD3 in the presence of 10 nmol/L of respective test constructs. Changes in cell impedance mediated by RKO cells were measured over time. Data are normalized to start of the coculture with T cells. Specific lysis was calculated by normalizing the CI values of test molecules with the CI values of the IgG4 isotype control using the following formula: 100 − (normalized mean CI of the test molecule/normalized mean CI of isotype control) × 100. Results are shown as mean ± SEM. **B,** PBMCs were stimulated with a CEF peptide pool in the presence of indicated constructs and IFNγ secretion levels were measured after 48 hours. **C,** PBMCs were stimulated with a CEF peptide pool and further expanded for 12 days by adding 20 U/mL IL2 on days 2, 5, and 7. On day 12, cells were collected and equally distributed to assay plates following a restimulation with a CEF peptide pool in the presence of indicated constructs. IFNγ secretion levels were measured after 48 hours. Constructs were added at 5 nmol/L. Data is shown as mean ± SEM and is exemplary for the three tested healthy blood donors. Significance was calculated using an unpaired one-way ANOVA with Holm–Sidak multiple comparisons test. n.s., not significant; h, hours.

enhanced the T-cell killing capacity superior as compared with single treatments or the combination of anti–4-1BB and PD-L1 mAbs (**Fig. 5A**).

PRS-344/S095012 stimulation supports antigen-specific T-cell response to antigen rechallenge

Given the strong proinflammatory and cytotoxic response of $CD8^+$ T cells observed upon stimulation with PRS-344/S095012, we aimed to further investigate its impact on antigen-specific T-cell responses. Tumor antigen-reactive T cells are expected to represent only a minor fraction of cells in the TME. To mimic this situation *in vitro*, we stimulated PBMCs from healthy donors with a pool of peptides from defined HLA class I-restricted T-cell epitopes from EBV, CMV, and influenza, and measured IFNγ secretion as common cytokine in antiviral responses.

20H4.9 alone or in combination with anti–PD-L1 mAb showed only limited effect on antigen-specific T-cell activation in this setting (**Fig. 5B**) while PRS-344/S095012 significantly increased the antigen-specific T-cell response. In a next step, we made use of an antigen reexposure model to mimic repetitive antigen stimulation in the TME. In this model, adding PRS-344/S095012 during antigen reexposure resulted in enhanced T-cell activation, which was significantly higher compared with the combination of anti–4-1BB and anti–PD-L1 mAbs or single treatments (**Fig. 5C**). These data validate the beneficial effect of PRS-344/S095012 on antigen-specific T-cell responses even after multiple rounds of antigen stimulation.

PRS-344/S095012 induces a strong antitumoral response *in vivo* and significantly increases survival

Finally, we investigated the antitumor effect of PRS-344/S095012 *in vivo*. Since PRS-344/S095012 is not cross-reactive to murine 4-1BB and PD-L1 (data not shown), we utilized a previously described hu4-1BB KI mouse model (30) subcutaneously implanted with MC38-huPD-L1 carcinoma cells. Treatment with PRS-344/S095012 resulted in a significant and dose-dependent tumor growth inhibition (TGI; **Fig. 6A**; Supplementary Table S2). In contrast, treatment with equimolar doses of the anti–PD-L1 mAb building block did not decrease tumor growth compared with vehicle control indicating that this model is resistant to anti–PD-L1 treatment. Furthermore, we observed complete tumor regression in 5 out of 10 mice at the 10 mg/kg PRS-344/S095012 dose level as well as significantly enhanced overall survival, with all animals in this treatment group surviving until study end at day 50 (**Fig. 6B** and **C**). The analysis of plasma samples from a satellite study revealed that s4-1BB was detected as early as 2 hours after the first administration of 10 mg/kg of PRS-344/S095012. Levels of s4-1BB plateaued after the third dose and were detectable until the end of the experiment in mice with complete and partial responses (**Fig. 6D**). This indicates that 4-1BB agonism with PRS-344/S095012 induces the release of s4-1BB in a dose-dependent manner in this model.

Discussion

While checkpoint inhibition with anti–PD-1/-PD-L1 mAbs has achieved durable clinical responses in certain patient populations, there is still a significant unmet need due to e.g., checkpoint refractory or resistant patients. Therefore, novel agents are required to increase the number of patients and indications benefiting from immunotherapy. Targeting the 4-1BB pathway offers an approach for enhancing T-cell reactivity against tumor-derived neoantigens, which can be combined with checkpoint blockade to simultaneously prevent their inhibition within the TME.

4-1BB, like other human TNFR superfamily members, requires the binding of homotrimeric ligand as a minimal unit for receptor clustering leading to activation (31). 4-1BBL is expressed on activated APCs (32) and can be proteolytically cleaved into a soluble trimeric ligand. It has been demonstrated that the soluble trimeric ligand is not an effective 4-1BB agonist due to limited cross-linking of 4-1BB, providing evidence that hyperclustering of 4-1BB on the cell surface is required to induce sufficient intracellular signaling (22, 33, 34). Bivalent anti-4-1BB mAbs can mediate hyperclustering by the binding of the Fc domain to FcγR-expressing cells, especially to the inhibitory FcγRIIb (27, 35). In addition to urelumab and utomilumab, further agonistic anti-4-1BB mAbs have entered clinical development (NCT04144842, NCT03881488, NCT03707093), all relying on FcγR-dependent clustering. The limitations of this approach include undesirable toxicity associated with FcγR interactions in the liver (36) as well as suboptimal efficacy hampered by differential FcγR expression levels and polymorphisms. Furthermore, FcγRIIb engagement has been described to reduce efficacy of several mAbs, including anti–PD-1 mAbs, potentially through FcγRIIb-mediated internalization (37, 38). To gain tumor specificity while remaining independent of FcγR interaction-associated limitations, FcγR-silenced bispecific molecules have been designed, inducing potent 4-1BB signaling by hyperclustering through binding to a tumor-localized target. This includes bispecific constructs targeting HER2 (23), fibroblast activation protein (FAP; NCT04049903), CD19 (36), or PD-L1 (NCT03917381, NCT04937153, NCT03809624, NCT04740424, NCT04762641, NCT03922204, NCT04442126; ref. 39) which are currently in preclinical or clinical development.

In the work reported within, we describe the preclinical characterization of the FcγR-silenced PD-L1/4-1BB bispecific molecule PRS-344/S095012, whose anticipated mode of action (MoA) is versatile and synergistic. The molecule is designed to (i) mediate blockade of the PD-1/PD-L1 pathway; (ii) provide a stimulation burst to antigen-specific 4-1BB-expressing TILs; (iii) localize 4-1BB activity to the TME, maximizing the therapeutic window; and (iv) combine checkpoint blockade with 4-1BB T-cell costimulation, preferentially on the same cell. This multi-layered MoA is achieved by bridging $4\text{-}1BB^+$ immune cells and PD-L1–expressing tumor cells or myeloid cells including myeloid-derived suppressor cells (MDSC) in the TME (40) or, potentially, APCs in the tumor draining lymph node (TDLN; refs. 41, 42).

The rationale to combine PD-1/PD-L1 and 4-1BB modulation is supported by previous preclinical studies demonstrating the synergistic effect of both pathways on antitumor immune responses (8, 43). Further evidence is provided by single-cell RNA sequencing data demonstrating enrichment of 4-1BB and PD-1 in $CD8^+$ T cells with an exhausted phenotype (44, 45) and that 4-1BB agonism can reinvigorate exhausted $CD8^+$ TILs (9).

In this present study, we demonstrated that PRS-344/S095012 not only mediates effective checkpoint blockade comparable with the anti–PD-L1 mAb atezolizumab, but also induces potent 4-1BB costimulation. PRS-344/S095012-mediated 4-1BB costimulation was strictly dependent on the presence of PD-L1–expressing cells as well as simultaneous TCR stimulation by anti-CD3, SEB, or synthetic viral HLA peptides, demonstrating the molecule's ability to boost preactivated T cells in a PD-L1–dependent manner. Tumor-localized 4-1BB stimulation via PRS-344/S095012 is an effective mechanism to target tumor-specific T cells with the promise of an improved therapeutic window.

The preclinical activity of PRS-344/S095012 described in this manuscript demonstrates the synergistic impact of potentiating 4-1BB agonism and PD-1/PD-L1 blockade via a bispecific-mediated

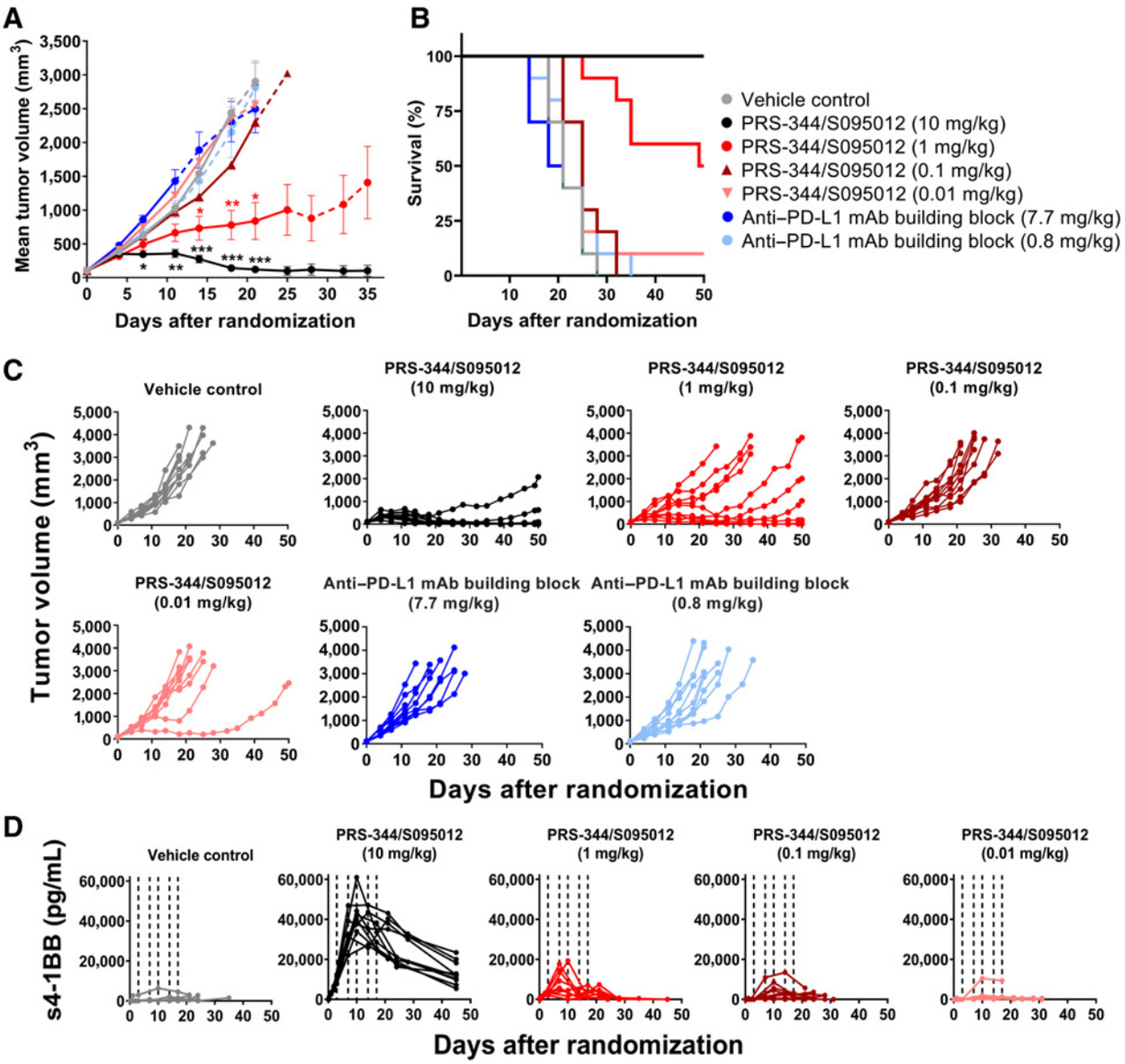

Figure 6.

PRS-344/S095012 drives potent *in vivo* antitumoral responses superior to PD-L1 blockade alone. Hu4-1BB KI were subcutaneously implanted with MC-38-huPD-L1 cells and treated with equimolar doses of constructs twice weekly for 3 weeks. **A,** Tumor volume was measured twice weekly and plotted as mean ± SEM. Dashed line indicates that at least one mouse in this group was sacrificed due to ethical considerations. **B,** Kaplan–Meier curves plotting the survival of all treated groups. **C,** Individual growth curves of the seven study groups. **D,** s4-1BB levels in the plasma of individual mice treated with the indicated molecules and doses. Dashed lines indicate treatment days. Data are representative of two independent studies. Kruskal–Wallis test with Dunn multiple comparisons test was performed to calculate significance.

MoA. *In vitro* assays confirmed superior efficacy of PRS-344/S095012 compared with anti–4-1BB or anti–PD-L1 mAbs, individually, but also to the combination of both mAbs, as evidenced by enhanced effector functions of $CD8^+$ and $CD4^+$ T cells, including the release of proinflammatory cytokine secretion and cytotoxicity. Different mechanisms likely contribute to the observed enhanced synergy and may be associated with the bispecific nature of PRS-344/S095012, like the ability of PRS-344/S095012 to bridge effector and target cells towards an optimal synapse. According to this hypothesis, the IFNγ released by PRS-344–/S095012-stimulated T cells can locally increase PD-L1 expression on tumor cells in *trans* and create a positive feedback loop, ultimately enhancing the activity of PRS-344/S095012 (46). At the same time, bridging of effector with target cells could stabilize the immunologic synapse, potentially enhancing activation and facilitating the killing of target cells (47). The latter hypothesis is supported by the data we generated in our T-cell killing experiments.

In a model mimicking antigen reexposure, we show that antigen-specific T cells benefit from stimulation with PRS-344/S095012. PRS-344/S095012 was superior to the combination of anti–4-1BB and anti–PD-L1 mAbs in enhancing the activation of T cells, rendering them

more responsive towards antigen challenge and, thus, leading to a strong increase in their proinflammatory response. At the same time, this data as well as preclinical results employing SEB and MLR experiments, suggest that PRS-344/S095012 could enhance the priming of novel tumor-specific T cells in TDLNs. PD-L1 which is expressed on APCs can mediate 4-1BB hyperclustering and stimulation of T cells, providing a synergistic feedback loop to increase the pool of tumor-reactive T cells benefitting from this intervention.

Using hu4-1BB KI mice, we demonstrated the capacity of PRS-344/S095012 to eradicate established human PD-L1$^+$ tumors, which were resistant to anti–PD-L1 treatment alone. One caveat of the model is that it is not suitable for an evaluation of toxicity as human PD-L1 expression is limited to the tumor site. Based on our *in vitro* data and previous publications (23), we anticipate that the T-cell compartment contributes to the antitumor response in this model. Nevertheless, it is likely that other immune cell populations, such as natural killer (NK) cells are also involved in 4-1BB agonist-driven antitumoral responses (48, 49). This is in line with clinical data from cinrebafusp alfa demonstrating NK cell expansion in the TME of patients (25).

We previously demonstrated with cinrebafusp alfa that HER2 tumor-localized 4-1BB agonism results in a favourable safety profile (25). As PD-L1 may be present in different human tissues beyond the tumor, including myeloid cells (41) as well as Kupffer cells and liver sinusoidal endothelial cells (LSEC; ref. 50), and hepatotoxicity in general remains a potential risk for any 4-1BB agonist, it is important to monitor liver function closely in clinical studies. For preclinical characterization of 4-1BB–mediated side effects humanized mouse models including a hu4-1BB/hu4-1BBL and huPD-1/huPD-L1 KI model, which also recapitulates human pattern of PD-L1 expression across all compartments, is required. To the best of our knowledge no mouse exists where the complete receptor and ligand pairs have been humanized for both pathways therefore the establishment of such models and the characterization of their suitability to address liver toxicity should be the focus of future research. While current preclinical models have been valuable in identifying the liver as a key organ to monitor 4-1BB agonism, the lack of translational relevance of currently available mouse models makes characterization of bispecifics more challenging. Models based on wild-type mice require use of a surrogate molecule that may have different properties from the drug candidate. Clinical data for one PD-L1/4-1BB bispecific indicate an emergence of some liver toxicity (albeit manageable; ref. 51), however this was not reported in their preclinical studies with a mouse surrogate (52). This is in line with earlier data from 4-1BB agonist antibodies which reported hepatic changes in mice only occurred at high doses, not necessarily aligning with clinical observations (30, 35). Humanized mouse models as outlined above may help overcome such shortcomings and facilitate better preclinical characterization of both safety and efficacy of PD-L1/4-1BB bispecifics, including a determination of therapeutic window.

S4-1BB is emerging as an interesting biomarker to assess 4-1BB agonism. To our knowledge, the data presented herein is the first preclinical report showing s4-1BB correlates with the dose and activity of an agonistic 4-1BB–targeting molecule. Different mechanisms have been described that may drive such release of s4-1BB including alternative splicing of 4-1BB transcripts (53, 54) or shedding from the cell surface by metalloproteases like ADAM17 (55). Our *in vitro* data showed that s4-1BB release is strongly enhanced in presence of a 4-1BB agonist but not by anti–PD-L1 treatment. Using control reagents, we also show that pathway agonism as opposed to mere 4-1BB binding is required for s4-1BB release. *In vivo* assessment demonstrated that mice with durable responses to PRS-344/S095012 had significantly elevated s4-1BB levels, suggesting that s4-1BB is indicative of the generation of an antitumoral response by PRS-344/S095012.

While future studies should elucidate the mechanism of s4-1BB and clinical implications such as impact on exposure levels, data from a recent clinical trial with cinrebafusp alfa, where s4-1BB concentrations were highest in patient cohorts obtaining clinical benefit, further highlight the clinical relevance and potential utility of s4-1BB as an exploratory biomarker (25).

4-1BB receptor hyperclustering by 4-1BBL or 4-1BB agonists including PD-L1/4-1BB bispecifics has been described to mediate receptor internalization, which enhances 4-1BB intracellular signaling (56, 57). A topic of future research could be to assess whether 4-1BB– and/or PD-L1–mediated internalization contributes to the MoA as described for PD-1/CTLA-4 bispecifics (58). The impact of PD-L1 expression levels and its modulation on PRS-344/S095012 activity is also of interest. A future biodistribution study in patients would help to characterize PRS-344/S095012 accumulation in PD-L1$^+$ tissues, and clinical consequences.

There are a number of PD-L1/4-1BB bispecifics in early clinical testing, for which preclinical data is available supporting PD-L1–dependent 4-1BB agonism. These bispecifics differ in terms of the bispecific technology, target binding affinity, differences between the affinity to the two targets, distance, valency, geometry, and Fc backbone as summarized in Supplementary Table S3 based on published data (39, 51, 57, 59–61).

PRS-344/S095012 uniquely utilizes an antibody-Anticalin fusion design in which the Anticalin protein is fused via a glycine-serine linker to the C-terminus of the antibody heavy chain resulting in bivalent binding towards both targets and providing the bispecific the required flexibility and distance to optimally stimulate T cells (as shown for cinrebafusp alfa/PRS-343; ref. 23). Other PD-L1/4-1BB bispecific technologies utilize single chain variable fragment (scFv) domains fused to the C- or the N-terminus of the Fc, or antibody arm exchange technologies to create heterodimeric bispecifics, with monovalent binders to each one of the targets. Since 4-1BBL is expressed as a homotrimer, with the natural 4-1BB/4-1BBL complex being a 3:3 multimer (62, 63), we hypothesize that bivalent bispecifics like PRS-344/S095012, that contain two binding moieties to 4-1BB, could favor the avidity-driven effective clustering of 4-1BB (64) which is essentially required to induce efficient intracellular signaling (33).

With the exception of one PD-L1/4-1BB bispecific molecule which has no Fc backbone but a human serum albumin (HSA) binding domain to extend half-life, all other PD-L1/4-1BB bispecifics contain a Fc backbone to increase half-life and stability, which is a silenced IgG1 backbone for all other competitor bispecifics. As a unique feature, PRS-344/S095012 was generated using an IgG4 backbone with F234A and L235A mutations, to further minimize the interaction with FcγRs and FcγR-mediated effector functions which are naturally reduced in the IgG4 format (65, 66). Using this backbone, we could also confirm the absence of FcγRIIb binding and resulting 4-1BB clustering which is required for anti–4-1BB mAb activity but is also associated with unwanted liver toxicity (35, 67).

Although most PD-L1/4-1BB bispecifics present KD values within the low nanomolar range ($KD_{4\text{-}1BB}$ = 0.15–13.8 nmol/L; $KD_{PD\text{-}L1}$ = 0.007–3.1 nmol/L), the bispecifics differ in their relative affinity difference between the anti–PD-L1 and the anti–4-1BB arm, that varies from 1 up to 69 (Ratio $KD_{4\text{-}1BB}/KD_{PD\text{-}L1}$). PRS-344/S095012 presents a relative affinity difference of 7, with a higher affinity to PD-L1, potentially driving the biodistribution of the drug to PD-L1–high environments like the tumor (68). Furthermore, it has been demonstrated in an assay format, that maximizes target bioavailability, that

higher affinity to PD-L1 compared with 4-1BB favors the optimal stimulation of T cells *in vitro* (61). However, data from patients will educate whether this translates into the clinical setting, since in patients, T-cell stimulation might be further impacted by other factors such as the density, dynamic expression, and internalization events of both targets (58, 68).

The ongoing clinical trials will shed more light on the contribution of all these variables to enhance T-cell activation, reduce toxicity, and significantly improve and extend the survival of patients with cancer.

In summary, we demonstrate that PRS-344/S095012 is potentiating T-cell function beyond the activity of mAbs targeting PD-L1 or 4-1BB, individually or in combination. Furthermore, PRS-344/S095012 offers the advantage of localizing 4-1BB agonism to a PD-L1$^+$ TME and PD-L1$^+$ TDLN. With these combined features, PRS-344/S095012 offers the promise of an improved therapeutic window relative to systemic 4-1BB agonists while focusing immune cell stimulation to the TME. Based on the preclinical data that demonstrates activity of PRS-344/S095012 in a mouse model resistant to anti–PD-L1 treatment, we suggest clinical evaluation of PRS-344/S095012 in patients whose cancer are resistant or refractory to checkpoint inhibitors. Since 4-1BB pathway activation offers an approach for enhancing tumor-specific T-cell responses, clinical evaluation in patients with heterogenous PD-L1 expression levels could be of interest. In addition, we provide for the first time preclinical *in vitro* and *in vivo* evidence using a PD-L1/4-1BB bispecific showing that s4-1BB is a potential biomarker to follow 4-1BB agonism in patients. Overall, we provide preclinical evidence for the synergistic effect of combining PD-1/PD-L1 blockade with target-dependent 4-1BB costimulation within a single molecule, supporting the progression of PRS-344/S095012 to clinical testing.

Authors' Disclosures

J.K. Peper-Gabriel reports a patent for WO 2020/025659 A1 pending; in addition, J.K. Peper-Gabriel is an employee of Pieris Pharmaceuticals GmbH. M. Pavlidou reports a patent for WO 2020/025659 A1 pending; in addition, M. Pavlidou is an employee of Pieris Pharmaceuticals GmbH. L. Pattarini reports a patent for WO 2020/025659 A1 pending. A. Morales-Kastresana is a full-time employee of Pieris Pharmaceuticals GmbH. T.J. Jaquin is an employee of Pieris Pharmaceuticals GmbH. E.-M. Hansbauer is an employee of Pieris Pharmaceuticals GmbH. H. Lelievre is employee of Institut de Recherches Servier. A. Scholer-Dahirel reports a patent for WO 2020/025659 A1 pending; in addition, A. Scholer-Dahirel is an employee of Institut de Recherches Internationales Servier. M. Zettl was an employee of Pieris Pharmaceuticals GmbH at the time the work was published in this article. R.S. Bel Aiba reports a patent for WO 2020/025659 A1 pending; in addition, R.S. Bel Aiba is an employee of Pieris Pharmaceuticals GmbH. C. Rothe reports a patent for WO 2020/025659 A1 pending; in addition, C. Rothe is a employee of Pieris Pharmaceuticals GmbH. S.A. Olwill reports a patent for WO 2020/025659 A1 pending to Pieris Pharmaceuticals GmbH. No disclosures were reported by the other authors.

Authors' Contributions

J.K. Peper-Gabriel: Conceptualization, resources, formal analysis, supervision, investigation, methodology, writing–original draft, writing–review and editing. **M. Pavlidou:** Conceptualization, resources, formal analysis, supervision, investigation, writing–original draft, project administration, writing–review and editing. **L. Pattarini:** Conceptualization, resources, formal analysis, supervision, methodology, writing–original draft, writing–review and editing. **A. Morales-Kastresana:** Formal analysis, writing–original draft, writing–review and editing. **T.J. Jaquin:** Supervision, writing–review and editing. **C. Gallou:** Supervision, writing–review and editing. **E.-M. Hansbauer:** Resources, formal analysis, investigation, methodology, writing–original draft, writing–review and editing. **M. Richter:** Formal analysis, investigation, writing–review and editing. **H. Lelievre:** Formal analysis, writing–review and editing. **A. Scholer-Dahirel:** Supervision, project administration, writing–review and editing. **B. Bossenmaier:** Conceptualization, supervision, project administration, writing–review and editing. **C. Sancerne:** Investigation. **M. Riviere:** Investigation. **M. Grandclaudon:** Formal analysis, methodology, writing–review and editing. **M. Zettl:** Supervision, writing–review and editing. **R.S. Bel Aiba:** Formal analysis, writing–review and editing. **C. Rothe:** Conceptualization, formal analysis, writing–review and editing. **V. Blanc:** Conceptualization, writing–review and editing. **S.A. Olwill:** Conceptualization, formal analysis, investigation, writing–original draft, writing–review and editing.

Acknowledgments

The research funding was provided by Pieris Pharmaceuticals GmbH and Institute de Recherches Servier.

We thank the extended Pieris Pharmaceuticals GmbH and Institute de Recherches Servier team for their support in generating and reviewing data related to this project. Especially we want to thank Marlon Hinner and Louis Matis for their support in generating the concept, as well as Christina Grasmüller, Katharina Köppe, Miriam Schaub, Linda Schnapp, Markus Rehle, Nicole Andersen, Michael Birkner, and Nicolas Quilitz for excellent technical support; Glenn Gauderat for the discussions; and Richa Bharti for biostatistical support.

The publication costs of this article were defrayed in part by the payment of publication fees. Therefore, and solely to indicate this fact, this article is hereby marked "advertisement" in accordance with 18 USC section 1734.

Note

Supplementary data for this article are available at Clinical Cancer Research Online (http://clincancerres.aacrjournals.org/).

Received July 30, 2021; revised September 25, 2021; accepted February 2, 2022; published first February 4, 2022.

References

1. Robert C, Schachter J, Long G, Arance A, Grob J, Mortier L, et al. Pembrolizumab versus ipilimumab in advanced melanoma. N Engl J Med 2015;372:2521–32.
2. Garon EB, Rizvi NA, Hui R, Leighl N, Balmanoukian AS, Eder JP, et al. Pembrolizumab for the treatment of non–small-cell lung cancer. N Engl J Med 2015;372:2018–28.
3. Rosenberg JE, Hoffman-Censits J, Powles T, van der Heijden MS, Balar AV, Mecchi A, et al. Atezolizumab in patients with locally advanced and metastatic urothelial carcinoma who have progressed following treatment with platinum-based chemotherapy: a single arm, phase 2 trial. Lancet 2016;387:1909–20.
4. Kwon BS, Weissman SM. cDNA sequences of two inducible T-cell genes. Proc Natl Acad Sci U S A 1989;86:1963–7.
5. Hurtado JC, Kim YJ, Kwon BS. Signals through 4-1BB are costimulatory to previously activated splenic T cells and inhibit activation-induced cell death. J Immunol 1997;158:2600–9.
6. Lee H-W, Park S-J, Choi BK, Kim HH, Nam K-O, Kwon BS. 4-1BB promotes the survival of CD8 + T lymphocytes by increasing expression of Bcl-x L and Bfl-1. J Immunol 2002;169:4882–8.
7. Teijeira A, Garasa S, Etxeberria I, Gato-Cañas M, Melero I, Delgoffe GM. Metabolic consequences of T-cell costimulation in anticancer immunity. Cancer Immunol Res 2019;7:1564–9.
8. Menk AV, Scharping NE, Rivadeneira DB, Calderon MJ, Watson MJ, Dunstane D, et al. 4-1BB costimulation induces T cell mitochondrial function and biogenesis enabling cancer immunotherapeutic responses. J Exp Med 2018;215:1091–100.
9. Leem G, Park J, Jeon M, Kim E-S, Kim SW, Lee YJ, et al. 4-1BB co-stimulation further enhances anti-PD-1-mediated reinvigoration of exhausted CD39+ CD8 T cells from primary and metastatic sites of epithelial ovarian cancers. J Immunother Cancer 2020;8:e001650.
10. Wilcox RA, Tamada K, Flies DB, Zhu G, Chapoval AI, Blazar BR, et al. Ligation of CD137 receptor prevents and reverses established anergy of CD8+ cytolytic T lymphocytes in vivo. Blood 2004;103:177–84.
11. Harao M, Forget M-A, Roszik J, Gao H, Babiera GV, Krishnamurthy S, et al. 4-1BB–enhanced expansion of CD8 + TIL from triple-negative breast cancer unveils mutation-specific CD8 + T cells. Cancer Immunol Res 2017;5:439–45.

12. Melero I, Shuford WW, Newby SA, Aruffo A, Ledbetter JA, Hellström KE, et al. Monoclonal antibodies against the 4-1BB T-cell activation molecule eradicate established tumors. Nat Med 1997;3:682–5.
13. Melero I, Murillo O, Dubrot J, Hervás-Stubbs S, Perez-Gracia JL. Multi-layered action mechanisms of CD137 (4-1BB)-targeted immunotherapies. Trends Pharmacol Sci 2008;29:383–90.
14. Melero I, Hirschhorn-Cymerman D, Morales-Kastresana A, Sanmamed MF, Wolchok JD. Agonist antibodies to TNFR molecules that costimulate T and NK cells. Clin Cancer Res 2013;19:1044–53.
15. Maude SL, Frey N, Shaw PA, Aplenc R, Barrett DM, Bunin NJ, et al. Chimeric antigen receptor T cells for sustained remissions in leukemia. N Engl J Med 2014; 371:1507–17.
16. Kalos M, Levine BL, Porter DL, Katz S, Stephan A, Bagg A, et al. T cells with chimeric antigen receptors have potent antitumor effects. Sci Transl Med 2011;3: 1–21.
17. Segal NH, Logan TF, Hodi FS, McDermott D, Melero I, Hamid O, et al. Results from an integrated safety analysis of urelumab, an agonist anti-CD137 monoclonal antibody. Clin Cancer Res 2017;23:1929–36.
18. Fisher TS, Kamperschroer C, Oliphant T, Love VA, Lira PD, Doyonnas R, et al. Targeting of 4-1BB by monoclonal antibody PF-05082566 enhances T-cell function and promotes anti-tumor activity. Cancer Immunol Immunother 2012;61:1721–33.
19. Gopal AK, Levy R, Houot R, Patel SP, Popplewell L, Jacobson C, et al. First-in-human study of utomilumab, a 4-1BB/CD137 agonist, in combination with rituximab in patients with follicular and other CD20+ non-Hodgkin lymphomas. Clin Cancer Res 2020;26:2524–34.
20. Ascierto PA, Simeone E, Sznol M, Fu YX, Melero I. Clinical experiences with anti-CD137 and anti-PD1 therapeutic antibodies. Semin Oncol 2010;37: 508–16.
21. Segal NH, He AR, Doi T, Levy R, Bhatia S, Pishvaian MJ, et al. Phase I study of single-agent utomilumab (PF-05082566), a 4-1BB/CD137 agonist, in patients with advanced cancer. Clin Cancer Res 2018;24:1816–23.
22. Li Y, Tan S, Zhang C, Chai Y, He M, Zhang CWH, et al. Limited cross-linking of 4-1BB by 4-1BB ligand and the agonist monoclonal antibody utomilumab. Cell Rep 2018;25:909–20.
23. Hinner MJ, Bel Aiba RS, Jaquin TJ, Berger S, Dürr MC, Schlosser C, et al. Tumor-localized costimulatory T-cell engagement by the 4-1BB/HER2 bispecific antibody-anticalin fusion PRS-343. Clin Cancer Res 2019;25:5878–89.
24. Rothe C, Skerra A. Anticalin® proteins as therapeutic agents in human diseases. BioDrugs 2018;32:233–43.
25. Piha-Paul S, Bendell JC, Tolcher A, Shroff R, Pohlmann PR, Hurvitz SA, et al. Abstract CT017: Clinical and biomarker activity of PRS-343, a bispecific fusion protein targeting 4-1BB and HER2, from a phase 1 study in patients with advanced solid tumors (Study PRS-343-PCS_04_16). Cancer Res 2021;81: CT017.
26. Jure-Kunkel M, Hefta LJ, Santoro M, Ganguly S, Halk EL, inventors; Bristol-Myers Squibb Co, assignee. Fully human antibodies against human 4-1BB. United States patent US7288638B2. 2007Oct 10.
27. Eskiocak U, Guzman W, Wolf B, Cummings C, Milling L, Wu HJ, et al. Differentiated agonistic antibody targeting CD137 eradicates large tumors without hepatotoxicity. JCI Insight 2020;5:e133647.
28. Lewis KB, Meengs B, Bondensgaard K, Chin L, Hughes SD, Kjær B, et al. Comparison of the ability of wild type and stabilized human IgG4 to undergo Fab arm exchange with endogenous IgG4 in vitro and in vivo. Mol Immunol 2009;46: 3488–94.
29. Vafa O, Gilliland GL, Brezski RJ, Strake B, Wilkinson T, Lacy ER, et al. An engineered Fc variant of an IgG eliminates all immune effector functions via structural perturbations. Methods 2014;65:114–26.
30. Qi X, Li F, Wu Y, Cheng C, Han P, Wang J, et al. Optimization of 4-1BB antibody for cancer immunotherapy by balancing agonistic strength with FcγR affinity. Nat Commun 2019;10:2141.
31. Vanamee ÉS, Faustman DL. Structural principles of tumor necrosis factor superfamily signaling. Sci Signal 2018;11:eaao4910.
32. Pollok KE, Kim Y-J, Hurtado J, Zhou Z, Kim KK., Kwon BS. 4-1BB T-cell antigen binds to mature B cells and macrophages, and costimulates anti-μ-primed splenic B cells. Eur J Immunol 1994;24:367–74.
33. Rabu C, Quéméner A, Jacques Y, Echasserieau K, Vusio P, Lang F. Production of recombinant human trimeric CD137L (4-1BBL): Cross-linking is essential to its T cell co-stimulation activity. J Biol Chem 2005;280:41472–81.
34. Wajant H. Principles of antibody-mediated TNF receptor activation. Cell Death Differ 2015;22:1727–41.
35. Ho SK, Xu Z, Thakur A, Fox M, Tan SS, DiGiammarino E, et al. Epitope and Fc-mediated crosslinking, but not high affinity, are critical for antitumor activity of CD137 agonist antibody with reduced liver toxicity. Mol Cancer Ther 2020;19:1040–51.
36. Claus C, Ferrara C, Xu W, Sam J, Lang S, Uhlenbrock F, et al. Tumor-targeted 4-1BB agonists for combination with T cell bispecific antibodies as off-the-shelf therapy. Sci Transl Med 2019;11:eaav5989.
37. Dahan R, Sega E, Engelhardt J, Selby M, Korman AJ, Ravetch JV. FcγRs modulate the anti-tumor activity of antibodies targeting the PD-1/PD-L1 axis. Cancer Cell 2015;28:285–95.
38. Teige I, Mårtensson L, Frendéus BL. Targeting the antibody checkpoints to enhance cancer immunotherapy – focus on FcγRIIB. Front Immunol 2019; 10:481.
39. Lakins MA, Koers A, Giambalvo R, Munoz-Olaya J, Hughes R, Goodman E, et al. FS222, a CD137/PD-L1 tetravalent bispecific antibody exhibits low toxicity and anti-tumor activity in colorectal cancer models. Clin Cancer Res 2020;26:4154–67.
40. Lu C, Redd PS, Lee JR, Savage N, Liu K. The expression profiles and regulation of PD-L1 in tumor-induced myeloid-derived suppressor cells. Oncoimmunology 2016;5:1–13.
41. Fransen MF, Schoonderwoerd M, Knopf P, Camps MGM, Hawinkels LJAC, Kneilling M, et al. Tumor-draining lymph nodes are pivotal in PD-1/PD-L1 checkpoint therapy. JCI Insight 2018;3:e124507.
42. Dammeijer F, van Gulijk M, Mulder EE, Lukkes M, Klaase L, van den Bosch T, et al. The PD-1/PD-L1-checkpoint restrains T cell immunity in tumor-draining lymph nodes. Cancer Cell 2020;38:685–700.
43. Palazón A, Martínez-Forero I, Teijeira A, Morales-Kastresana A, Alfaro C, Sanmamed MF, et al. The HIF-1α hypoxia response in tumor-infiltrating T lymphocytes induces functional CD137 (4-1BB) for immunotherapy. Cancer Discov 2012;2:608–23.
44. Zheng C, Zheng L, Yoo J-K, Guo H, Zhang Y, Guo X, et al. Landscape of infiltrating T cells in liver cancer revealed by single-cell sequencing. Cell 2017;169:1342–56.
45. Guo X, Zhang Y, Zheng L, Zheng C, Song J, Zhang Q, et al. Global characterization of T cells in non-small-cell lung cancer by single-cell sequencing. Nat Med 2018;24:978–85.
46. Taube JM, Anders RA, Young GD, Xu H, Sharma R, Mcmiller TL, et al. Colocalization of inflammatory response with B7-H1 expression in human melanocytic lesions supports an adaptive resistance mechanism of immune escape. Sci Transl Med 2012;4:127ra37.
47. Otano I, Azpilikueta A, Glez-Vaz J, Alvarez M, Medina-Echeverz J, Cortés-Domínguez I, et al. CD137 (4-1BB) costimulation of CD8+ T cells is more potent when provided in cis than in trans with respect to CD3-TCR stimulation. Nat Commun 2021;12:7296.
48. Wilcox RA, Tamada K, Strome SE, Chen L. Signaling through NK cell-associated CD137 promotes both helper function for CD8+ cytolytic T cells and responsiveness to IL-2 but not cytolytic activity. J Immunol 2002;169:4230–6.
49. Melero I, Johnston JV, Shufford WW, Mittler RS, Chen L. NK1.1 cells express 4-1BB (CDw137) costimulatory molecule and are required for tumor immunity elicited by anti-4-1BB monoclonal antibodies. Cell Immunol 1998;190: 167–72.
50. Kassel R, Cruise MW, Iezzoni JC, Taylor NA, Pruett TL, Hahn YS. Chronically inflamed livers up-regulate expression of inhibitory B7 family members. Hepatology 2009;50:1625–37.
51. Garralda E, Geva R, Ben-Ami E, Maurice-Dror C, Calvo E, LoRusso P, et al. First-in-human phase I/IIa trial to evaluate the safety and initial clinical activity of DuoBody®-PD-L1 × 4-1BB (GEN1046) in patients with advanced solid tumors. J Immunother Cancer 2020;8:A250–1.
52. Muik A, Altintas I, Gieseke F, Salcedo T, Burm S, Diken M, et al. Fc-silenced bispecific antibodies targeting PD-L1 and 4-1BB combine checkpoint blockade and T-cell co-stimulation to promote anti-tumor activity [abstract]. In: Proceedings of the 34th Annual Meeting & Pre-Conference Programs (SITC 2019); 2019Nov 6—10; National harbor, MD. Hoboken (NJ). J Immunother Cancer; 2019. Abstr nr P609.
53. Labiano S, Palazón A, Bolaños E, Azpilicueta A, Sánchez-Paulete AR, Morales-Kastresana A, et al. Hypoxia-induced soluble CD137 in malignant cells blocks CD137L-costimulation as an immune escape mechanism. J Immunother Cancer 2016;5:e1062967.
54. Luu K, Shao Z, Schwarz H. The relevance of soluble CD137 in the regulation of immune responses and for immunotherapeutic intervention. J Leukoc Biol 2019; 107:731–8.
55. Nielsen MA, Andersen T, Etzerodt A, Kragstrup TW, Rasmussen TK, Stengaard-Pedersen K, et al. A disintegrin and metalloprotease-17 and galectin-9 are

important regulators of local 4-1BB activity and disease outcome in rheumatoid arthritis. Rheumatol 2016;55:1871–9.
56. Martinez-Forero I, Azpilikueta A, Bolanos-Mateo E, Nistal-Villan E, Palazon A, Teijeira A, et al. T cell costimulation with anti-CD137 monoclonal antibodies is mediated by K63-polyubiquitin-dependent signals from endosomes. J Immun. 2013;190:6694–706.
57. Geuijen C, Tacken P, Wang L-C, Klooster R, van Loo PF, Zhou J, et al. A human CD137×PD-L1 bispecific antibody promotes anti-tumor immunity via context-dependent T cell costimulation and checkpoint blockade. Nat Commun 2021; 12:4445.
58. Dovedi SJ, Elder MJ, Yang C, Sitnikova SI, Irving L, Hansen A, et al. Design and efficacy of a monovalent bispecific PD-1/CTLA4 antibody that enhances CTLA4 blockade on PD-1+ activated T cells. Cancer Discov 2021;11:1100–17.
59. Snell D, Gunde T, Warmuth S, Lichtlen P, Tietz J, Brock M, et al. Abstract 2276: Preclinical development and mechanism of action studies of NM21–1480, a PD-L1/4-1BB/HSA trispecific MATCH3 therapeutic clinical candidate. Cancer Res 2020;80:2276.
60. Jeong S, Park E, Kim H-D, Sung E, Kim H, Jeon J, et al. Novel anti-4- antibody augments anti-tumor immunity through tumor-directed T-cell activation and checkpoint blockade. J Immunother Cancer 2021;9:e002428.
61. Warmuth S, Gunde T, Snell D, Brock M, Weinert C, Simonin A, et al. Engineering of a trispecific tumor-targeted immunotherapy incorporating 4-1BB co-stimulation and PD-L1 blockade. Oncoimmunology 2021;10:1.
62. Gilbreth RN, Oganesyan VY, Amdouni H, Novarra S, Grinberg L, Barnes A, et al. Crystal structure of the human 4-1BB/4-1BBL complex. J Biol Chem 2018;293: 9880–91.
63. Chin SM, Kimberlin CR, Roe-Zurz Z, Zhang P, Xu A, Liao-Chan S, et al. Structure of the 4-1BB/4-1BBL complex and distinct binding and functional properties of utomilumab and urelumab. Nat Commun 2018;9: 4679.
64. Vauquelin G, Charlton SJ. Exploring avidity: understanding the potential gains in functional affinity and target residence time of bivalent and heterobivalent ligands. Br J Pharmacol 2013;168:1771–85.
65. Bruhns P, Iannascoli B, England P, Mancardi DA, Fernandez N, Jorieux S, et al. Specificity and affinity of human Fcγ receptors and their polymorphic variants for human IgG subclasses. Blood 2009;113:3716–25.
66. Brüggemann M, Williams GT, Bindon CI, Clark MR, Walker MR, Jefferis R, et al. Comparison of the effector functions of human immunoglobulins using a matched set of chimeric antibodies. J Exp Med 1987;166:1351–61.
67. Xu Y, Szalai AJ, Zhou T, Zinn KR, Chaudhuri TR, Li X, et al. FcγRs modulate cytotoxicity of anti-fas antibodies: implications for agonistic antibody-based therapeutics. J Immunol 2003;171:562–8.
68. Bensch F, van der Veen EL, Lub-de Hooge MN, Jorritsma-Smit A, Boellaard R, Kok IC, et al. 89Zr-atezolizumab imaging as a non-invasive approach to assess clinical response to PD-L1 blockade in cancer. Nat Med 2018;24: 1852–8.